Low-dose pyrrolidine dithiocarbamate/copper complex induces lung epithelial cell apoptosis via the mitochondria- and ER-stress-related signaling pathways

Ya-Wen Chen[*,Δ], Kuo-Liang Chen[#], Chun-Hung Chen[**,¶], Hsi-Chin Wu[#], Chin-Chuan Su[##], Chin-Ching Wu[ξ], Tzong-Der Way[§], Dong-Zong Hung[¶,$], Cheng-Chien Yen[†], Yuan-Ting Yang[¶], Tien-Hui Lu[¶]

[*]Department of Physiology, and Graduate Institute of Basic Medical Science, College of Medicine, China Medical University, Taichung, Taiwan 404

[#]Department of Urology, China Medical University Hospital, Taichung, Taiwan 404

[**]Department of Emergency, China Medical University Hospital, Taichung, Taiwan 404

[##]Department of Otorhinolaryngology, Head and Neck Surgery, Changhua Christian Hospital, Changhua, Taiwan 500

[ξ]Department of Pulic Health, China Medical University, Taichung, Taiwan 404

[§]Department of Biological Science and Technology, College of Life Sciences, China Medical University, Taichung, Taiwan 404

[¶]Graduate Institute of Drug Safety, College of Pharmacy, China Medical University, Taichung, Taiwan 404

[$]Toxicology Center, China Medical University Hospital, Taichung, Taiwan 404

[†]Department of Occupational Safety and Health, College of Health Care and Management, Chung Shan Medical University, Taichung, Taiwan 402

Running title: PDTC/Cu complex induces lung epithelial cell apoptosis

Table of Contents Graphic

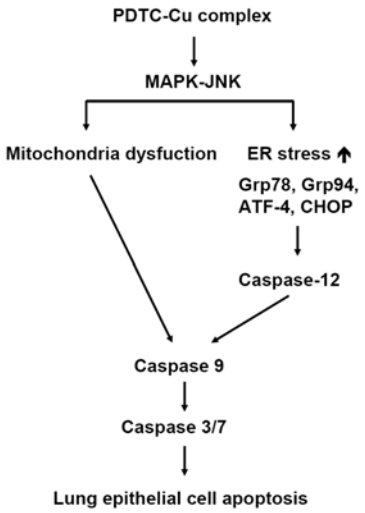

Abstract

Pyrrolidine dithiocarbamate (PDTC) is widely used in pesticides, fungicides, insecticides, and herbicides. Copper (Cu) is a toxic heavy metal in the environment, and an essential trace metal element in the body, which is involved in many biological processes as a catalytic cofactor. The present study is designed to investigate the cellular toxicity of low-dose PDTC, $CuCl_2$, and PDTC/Cu complex exposure in lung alveolar epithelial cells that serve primary structural and functional roles in the lungs. The results showed that PDTC or $CuCl_2$ alone did not affect cell viability, but PDTC/Cu complex significantly decreased lung alveolar epithelial cell viability. PDTC/Cu complex dramatically enhanced the phosphorylations of JNK and ERK proteins. PDTC/Cu complex did not affect the phosphorylation of p38 protein. PDTC/Cu complex was capable of activating the apoptosis-related caspases including caspase-9, caspase-7, and caspase-3, which could be reversed by the addition of JNK inhibitor SP600125 or transfection of MAPK8 short hairpin RNA. PDTC/Cu complex also increased cytosolic cytochrome c and decreased mitochondrial transmembrane potential. the Bcl-2 mRNA and protein expressions were decreased in lung epithelial cells treated with PDTC/Cu complex, which could be reversed by SP600125. Furthermore, PDTC/Cu complex could trigger the expressions of ER stress-associated signaling molecules including Grp78, Grp94, caspase-12, ATF4, and CHOP, which

could be reversed by SP600125. Taken together, these results indicate that exposure to low-dose PDTC/Cu complex induces cytotoxicity and apoptosis in alveolar epithelial cells via the mitochondria- and ER-stress-related signaling pathways.

Keywords: lung epithelial cells, PDTC, Cu, mitochondria, ER stress, apoptosis

Footnotes

[Δ]Author to whom first author and correspondence should be addressed: Ya Wen Chen, Department of Physiology, Graduate Institute of Basic Medical Science, College of Medicine, China Medical University, No.91 Hsueh-Shih Road, Taichung, 40402 Taiwan. Fax: + 886 4 22333641. E-mail: ywc@mail.cmu.edu.tw

Introduction

Recently, many studies have discussed the biological effects of dithiocarbamate-metal complexes because of their wide application in pesticides, fungicides, insecticides, and herbicides (*1*, *2*). Pyrrolidine dithiocarbamate (PDTC) is a low-molecular weight thiol compound that functions as a metal chelator and antioxidant. For example, PDTC demonstrated protective effects against paraquat-induced pulmonary damage (*3*). In addition, PDTC has been found to inhibit NF-κB and inflammatory cytokines, protecting against many diseases including obstructive uropathy and neuropathic disorders (*4*, *5*). Furthermore, PDTC has also been used in chelating therapy for metal intoxication (*6*). However, recent studies have shown that PDTC can induce cell death in several cell types (*7*, *8*), and toxic effects have been observed when PDTC is added to cultured HL-60 cells (*8*).

Copper (Cu) is an essential trace element that functions as a catalytic cofactor and is involved in many biological processes (*9*) and plays an important role in the oxidant defense system (*10*). However, Cu is also present in our environment, and an excess of Cu may have adverse effects on our health (*8*). Cu overload may lead to the generation of unbound ionic Cu^{2+}, inducing hydroxyl radicals, oxidative stress, and displacement of other essential metal cofactors from metalloenzymes. The recommended amount of dietary intake of Cu is 20 μg/kg body weight per day for

adults and 50 μg/kg body weight per day for infants (*10*). Blood is an important target of drug exposure and environmental chemicals (*8*), and previous studies have shown that chronic exposure to high doses of Cu (e.g., 200 μg/g in pigs) can lead to gastrointestinal damage, liver cirrhosis, hemolysis, and damage to renal tubules and the central nervous system (*11*). Another report has also indicated that excessive Cu accumulation (1 g/L in drinking water) decreases superoxide dismutase (SOD) activity and glutathione (GSH) levels and increases malondialdehyde (MDA) concentrations in brain tissues (*12*). Because PDTC is widely used in agriculture and Cu is present throughout the environment, chronic exposure both PDTC and Cu is likely.

The lungs receive most of the venous bloodstream and implements blood-air exchange. Previous studies have not explored PDTC, Cu, or PDTC/Cu complex toxicity in lung epithelial cells. Thus, we used lung cells to investigate the consequences of exposure to PDTC, Cu, and PDTC/Cu complex. Lung epithelial apoptosis has been demonstrated in several lung functional disorders and diseases, such as lung fibrosis (*13*), emphysema (*14*), and acute lung injury (*15*).

Mitogen-activated protein kinase (MAPK) pathways are involved in lung inflammation and injury, including idiopathic pulmonary fibrosis (*16*). A previous study has reported that MAPKs are conserved enzymes that connect cell surface

receptors to critical regulatory targets within the cell and respond to chemical and physical stresses (*17*). There are three major groups of MAPKs, including extracellular signal-regulated kinase (ERK)-1/2, c-jun N-terminal kinase (JNK)-1/2/3, and p38 MAPK. JNK and p38 are involved in apoptotic signaling Yoshida *et al.*, (*16*), and Penna *et al.* (*18*) demonstrated that endoplasmic reticulum (ER) stress can enhance phosphorylation of eIF2alpha and JNK during apoptotic signaling.

The ER is responsible for the synthesis, folding, assembly, and modification of cytoplasmic and membrane proteins (*19*). Activation of the ER stress response upregulates ER resident chaperones and other regulatory components of the secretary pathway. Previous studies have reported that under stress conditions, unfolded proteins accumulate in the ER and sequester Grp78, preventing the secretion of incompletely assembled immunoglobulins. This causes release of activating transcription factor 6 (ATF6), PERK, and IRE-1, promoting their activity. Enhanced ER stress also leads to a decrease in the inner mitochondrial transmembrane potential (MMP) and release of cytochrome *c* associated with the intrinsic apoptotic pathway (*20*). Cytochrome *c* binds to apoptotic protease activating factor 1 (Apaf-1) to form a cytochrome *c*-Apaf-a complex. In the presence of ATP or dATP, this complex recruits and activates procaspase-9, which then activates other caspases (*21*).

The lungs provide blood-air exchange for the body, and lung epithelial cells

compose the alveolar wall that facilitates this exchange. In this study, we evaluated the toxicity of the environmental pollutants PDTC, $CuCl_2$, and PDTC/Cu complex in lung epithelial cells and found that PDTC/Cu complex likely promotes cytotoxicity by induction of apoptosis.

Materials and Methods

Cell line. Rat lung epithelial-derived L2 cells (CCL-149) were purchased from ATCC. Cells were cultured in a humidified chamber with a 5% CO_2/95% air mixture at 37 °C. Cells were maintained in RPMI 1640 medium supplemented with 10% fetal bovine serum (FBS) containing 1% penicillin-streptomycin (Gibco/Invitrogen, Carlsbad, CA, USA).

Cell viability assay. Cells were washed with PBS and detached from dishes using trypsin. They were then cultured in 24-well plates ($2x10^5$ cells/well) and treated with PDTC, $CuCl_2$, or PDTC/Cu complex for 24 h. After incubation, the medium was removed and replaced with fresh medium containing 30 μL of 2 mg/mL 3-(4,5-dimethyl thiazol-2-yl-)-2,5-diphenyl tetrazolium bromide (MTT). After incubation for 4 h, the medium was removed, and 1 mL of imethyl sulfoxide (Sigma, St. Louis, MO, USA) was added to dissolve the blue formazan crystals. Following mixing, 150 μL was transferred to a 96-well plate. An enzyme-linked immunosorbent assay reader (Thermo Fisher Scientific, Waltham, MA, USA) was used for fluorescence detection at a wavelength of 570 nm.

Intracellular copper concentration. To determine the copper levels in cells, cells

were culture in 10 cm^2 dishes and treated with indicated compounds for 24 h. Cells were harvested and placed in a 15ml polyethylene tube, and 0.5 ml of a 3:1 mixture of hydrochloric acid (35%) and nitric acid (70%) was added. The cell mixtures were heated at 50 ℃. After colling, the copper contents were determined by Inductively coupled plasma mass spectrometry (ICP-MS).

Plasmid and transfection. RNAi reagents were obtained from the National RNAi Core, Institute of Molecular Biology, and Genomic Research Center, Taiwan. A short hairpin RNA (shRNA) was designed to target the specific sequence of human MAPK8 (Clone ID: TRCN0000001056; target sequence: 5'-GCCCAGTAATATAGTAGTAAA-3'). The shRNA was transfected using Lipofectamine 2000 (Invitrogen, Carlsbad, CA, USA) according to the recommendations of the manufacturer. Before transfection, cells were seeded without antibiotics, and the efficiency of transfection (approximately 80%) was determined using an equal amount of a plasmid encoding the green fluorescent protein driven by the cytomegalovirus promoter.

Cytosol cytochrome c detection. Cells were homogenized with a pestle and mortar in 0.4 M mannitol, 25 mM MOPS (pH 7.8), 1 mM EGTA, 8 mM cysteine, and 0.1%

(w/v) bovine serum albumin (BSA). Cell debris was then removed via centrifugation at 6000 × g for 2 min. The supernatant was then removed and recentrifuged at 12000 × g for 15 min to pellet the mitochondria, and the supernatant (cytosol) was stored for Western blot analysis.

Western blot analysis. Cells were treated with the indicated compounds for various time periods. Afterwards, 50 μg of protein from each cell lysate was subjected to electrophoresis on 10% (w/v) SDS-polyacrylamide gels and transferred to polyvinylidene difluoride membranes. The membranes were then blocked in PBST (PBS and 0.05% Tween 20) containing 5% nonfat dry milk for 1 h. After blocking, the membrane was incubated with antibodies against p-JNK, JNK1, cytochrome *c*, caspase 9, caspase 3, caspase 12, Grp78, Grp94, and α tubulin (Santa Cruz Biotechnology, Santa Cruz, CA, USA). Membranes were then washed with 0.1% PBST and incubated with secondary antibodies conjugated to horseradish peroxidase for 45 min. The antibody-reactive bands were revealed using enhanced chemiluminescence reagents (Amersham Biosciences, Sweden) and exposed to radiographic film (Kodak, Rochester, NY, USA).

Quantitative real-time PCR. This method was performed as previously described

(*22*). L2 cells were treated with $CuCl_2$, PDTC, or PDTC/Cu complex for the indicated times, and total RNA was extracted. Total RNA (5 μg) was heated to 90°C for 5 min to remove any secondary structures and then rapidly placed on ice. Samples were then reverse transcribed into cDNA using AMV RTase (Promega, Madison, WI, USA) at 42 °C in reaction buffer containing 2.5 mM dNTPs, 40U/μL RNasin (Promega, Madison, WI, USA), 100 nmol random-hexamer primers, 1× RTase buffer; 30U AMV RTase in nuclease-free water at a final volume of 20 μL. The mixture was incubated at 42 °C for 60 min. Samples were then denatured at 95 °C for 10 min and placed on ice. Primers for rat Bcl-2, Grp78, Grp94, ATF4, and C/EBP homologous protein (CHOP) were as follows: Bcl-2 forward 5'-CTTTGTGGAACTGTACGGCCCCAGCATGCG-3' and reverse 5'-ACAGCCTGCAGCTTTGTTTCATG-GTACATC-3' (*23*), Grp78 forward 5'-TGATAATCAGCCCACCGTAACA-3' and reverse 5'-GGAGGGATTCCAGTCAGATCAA-3' (*24*), Grp94 forward 5'-AAGGTCATTGTCACGTCGAAA -3' and reverse 5'-GTGTTTCCTCTTGGGTCAGC-3' (*25*), ATF4 forward 5'-GTTGGTCAGTGCCTCAGACA -3' and reverse 5'-CATTCGAAACAGAGCATCGA-3' (*26*), CHOP forward 5'-CCAGCAGAGGTCACAAGCAC-3' and reverse 5'-

CGCACTGACCACTCTGTTTC-3' (*26*). Each sample was detected using real-time Sybr Green PCR reagent (Invitrogen, Carlsbad, CA, USA) with transgene-specific primers in a 25 μL reaction volume, and amplification was performed using an ABI Prism 7900HT real-time thermal cycler (Applied Biosystems, Carlsbad, CA, USA). Cycling conditions were 2 min at 50°C, 10 min at 95°C, 40 cycles of 92°C for 30 sec, and 60°C for 1 min. Real-time fluorescence detection was performed during the 60°C annealing/extension step of each cycle. Melt-curve analysis was performed on each primer set to ensure that no primer dimers or nonspecific amplification was present under the optimized cycling conditions. The fold difference in mRNA expression between treatment groups was determined using the relative quantification method utilizing real-time PCR efficiencies and normalized to the β-actin gene, thus comparing relative C_T changes between control and experimental samples. Prior to conducting statistical analyses, the fold change from the mean of the control group was calculated for each individual sample, including individual control samples to assess variability within the group.

MMP analysis. The detection of MMP was performed as previously described (*27*). After cells were treated with $CuCl_2$, PDTC, or PDTC/Cu complex, they were harvested at the indicated time points and washed twice with PBS. The cells were

then treated with 40 nM $DiOC_6$ for 30 min and analyzed in a FACScan flow cytometer (Becton Dickinson, Franklin Lakes, NJ, USA).

Statistical analysis. Data are presented as the means ± SEM. For comparison between two groups with one independent variable, significance was assessed using the paired Student's *t* test (Sigma Plot 10.0; Systat Software, San Jose, CA, USA). For two or more independent variables, one-way ANOVA was used for analysis, and Duncans's post hoc test was applied to identify group differences. A *P* value of less than 0.05 was considered significant. The statistical package SPSS 11.0 for Windows (SPSS Inc., Chicago, IL, USA) was used for the statistical analysis.

Results

Effects of PDTC, $CuCl_2$, and PDTC/Cu complex on cell viability, intracellular copper contents, MAPKs and caspase-9, -7 and -3 proteins expression in L2 alveolar epithelial cells. To examine the effects of PDTC, $CuCl_2$, and PDTC/Cu complex on lung alveolar epithelial cell viability, MTT assays were used to detect cytotoxicity in L2 cell. Cells were treated with various doses of $CuCl_2$ with or without PDTC (0, 0.5, or 1 μM) for 24 h. The results showed that the viability of cells was not altered in the PDTC or $CuCl_2$ treatment groups, but viability was decreased in cells treated with the PDTC/Cu complex (Figure 1). These experiments demonstrated that the PDTC/Cu complex might be cytotoxic to L2 cells.

Next experiments we found that exposed to PDTC/Cu complex resulted amount of copper accumulation in cells. However, there were low levels of copper in control, PDTC, and $CuCl_2$ groups. The levels of copper concentration was 7.65±1.95 (ng/mg protein), 10.14 ±0.18 (ng/mg protein), and 9.51±3.73 (ng/mg protein) in control, PDTC, and $CuCl_2$ groups, respectively. However, there was 210.08±39.81 (ng/mg protein) in PDTC/Cu complex administered cells (Figure 2).

To investigate the possible induction of apoptotic signaling, we determined the expression of caspase-9, caspase-7, and caspase-3 proteins in L2 cells following treatment with PDTC, $CuCl_2$, or PDTC/Cu complex. After cells were treated with

PDTC (0.5 μM) and $CuCl_2$ (1 μM) for 12, 14, or 16 h, the cleaved form of caspase-9 was significantly increased (Figure 3A). Furthermore, the cleaved forms of caspase-7 and caspase-3 were also increased after cells were treated with PDTC/Cu complex for 14, 16, and 24 h (Figure 3B and 3C).

Next experiments, MAPK signaling induced by the PDTC/Cu complex was evaluated by Western blot analysis. We further demonstrated PDTC/Cu complex dramatically enhanced pJNK and pERK proteins expression. These effects induced by PDTC/Cu complex could be inhibited by JNK inhibitor, SP600125, but not ERK inhibitor, PD98059 (Figure 4A and 4B). Besides, there are no effects on p38 protein expression (Figure 4C). A previous study reported that p-JNK plays an important role during the induction of the intrinsic mitochondrial apoptotic pathway (Dhanasekaran and Reddy, 2008). These results indicated that the cytotoxicity of PDTC/Cu complex might involve p-JNK protein regulation.

Next we determined if PDTC/Cu complex-induced cell death signaling required the p-JNK pathway. After cells were treated with PDTC/Cu complex, the cleaved form of caspase-9 was detected at 12h and the cleaved forms of caspase-7 and caspase-3 were detected at 24 h. Furthermore, this PDTC/Cu complex-induced caspase-9, caspase-7, and caspase-3 cleavage was reversed by addition of the JNK inhibitor, SP600125, or transfection with a MAPK8 shRNA (Figure 5A, 5B and 5C).

These results indicated that PDTC-Cu complex induced cell death via the p-JNK pathway.

Effects of PDTC, $CuCl_2$, and PDTC/Cu complex on Bcl-2 expression, MMP, and cytosolic cytochrome c release in L2 alveolar epithelial cells. To further investigate cell signaling in PDTC, $CuCl_2$, and PDTC/Cu complex treated L2 cells, we determined the effects of PDTC (0.5 μM), $CuCl_2$ (1 μM), and PDTC/Cu complex on Bcl-2 mRNA and protein expression. The results showed that PDTC and $CuCl_2$ did not alter Bcl-2 mRNA or protein expression. However, cells treated with PDTC/Cu complex demonstrated significantly decreased Bcl-2 mRNA and protein levels, and addition of the JNK inhibitor, SP600125, reversed these effects (Figure 6A-a and 6A-b). A previous study has shown that changes in expression of Bcl-2 family proteins correlated with decrease MMP and release of cytochrome *c* in arsenic-trioxide–induced cell apoptosis (*28*). Thus, we next investigated possible alterations in MMP and cytochrome *c* release in cells treated with PDTC, $CuCl_2$, or PDTC/Cu complex. The MMP did not change in PDTC or $CuCl_2$ treated cells. However, the MMP was significantly decreased in cells treated with PDTC/Cu complex (Figure 6B). Our results also showed that neither PDTC nor $CuCl_2$ induced cytochrome *c* release in L2 cells. However, cells treated with PDTC/Cu complex

demonstrated a dramatic increase in cytochrome *c* release (Figure 6C). The effects of PDTC/Cu complex on MMP and cytochrome *c* release were both reversed by addition of the JNK inhibitor, SP600125 (Figure 6B and 6C).

Effects of PDTC, $CuCl_2$, and PDTC/Cu complex on the ER stress pathway in L2 alveolar epithelial cells. We next investigated the role of the ER stress pathway in the cytotoxicity of PDTC/Cu complex in L2 cells. We first examined the expression of Grp78, Grp94, and procaspase-12 proteins by Western blot. Results showed that the Grp78 and Grp94 protein levels were significantly increased following 8–24 h of PDTC (0.5 μM) and Cu (1 μM) treatment. In contrast, procaspase-12 levels were decreased after treatment with PDTC/Cu complex for 8–24 h (Figure 7). Furthermore, mRNAs encoding proteins related to the ER stress pathway, including Grp78, Grp94, ATF4, and CHOP, were dramatically increased after cells were treated with PDTC/Cu complex, and these effects could be inhibited by addition of the JNK inhibitor, SP600125 (Figure 8A, 8B, 8C and 8D). These results indicated that PDTC/Cu complex induced ER stress signaling and that this effect required the p-JNK pathway in L2 cells.

Discussion

Many studies have reported that PDTC and $CuCl_2$ accumulation disrupt antioxidant systems and induced cell damage in many cell types. The effects of PDTC- and $CuCl_2$-induced cell damage have been related to the ROS-triggered apoptosis pathway (*8*). Despite many studies having reported on PDTC and $CuCl_2$ toxicity in several kinds of cells, there have been no studies that have discussed low-dose PDTC, $CuCl_2$, and PDTC/Cu complex toxicity in type-2 alveolar epithelial cells. Specifically, the precise action and mechanism of PDTC/Cu complex induced cell damage in alveolar epithelial cells have not been clarified. In the present study, we investigate the cytotoxicity of PDTC/Cu complex and its possible mechanisms of cell death in alveolar epithelial cells.

Apoptotic signaling is divided into two major cell-death pathways, including intrinsic and extrinsic pathways. A previous study showed that activation of intrinsic apoptotic signaling includes release of mitochondria cytochrome *c*, an increase in Apaf-1 expression, a decrease in pro-apoptotic Bcl-2 family proteins, and activation of caspases and cleavage of their cellular substrates. The extrinsic signaling pathway is mediated by death receptors and subsequent activation of the caspase cascade (*29*). Recently, it has been shown that alveolar epithelial cell death promotes the progression of pulmonary fibrosis (*30*). Type II alveolar epithelial cells are

responsible for surfactant synthesis and secretion (*31*). In our study, we found that treatment of cells with low-dose PDTC or $CuCl_2$ did not have any effect on cell viability. However, when cells were exposed to PDTC and $CuCl_2$ simultaneously, this PDTC/Cu complex significantly reduced the viability and activation of caspase-9, -7 and -3 in L2 cells. Therefore, these results indicated that formation of PDTC/Cu complex was cytotoxic to L2 cells. Furtheremore, PDTC/Cu complex induced apoptotic effects in L2 cells.

The MAPK/JNK signaling cascade promotes cell death in several cell types (*32, 33*). The MAPK pathway is known to be involved in many biology and physiology functions, such as proliferation, survival, differentiation, and locomotion. A total of nine MAPKs have been described in mammalian cells, including ERK1/2, ERK3, ERK4, ERK5, ERK6 /p38MAPKg, ERK7, ERK8, JNK1/2/3, and p38MAPKa/b/d. MAPKs are activated by a cascade of protein phosphorylation and can subsequently phosphorylate a large number of substrate proteins to regulate downstream of signaling (*34*). The JNKs belong to the superfamily of MAP kinases that are involved in many biological processes, including cell proliferation, differentiation, and apoptosis. Recently, studies have reported that JNKs can be activated by growth factors, cytokines, and stress factors. Thus, JNKs seems to play an important role in regulating apoptotic signaling (*35*). In our study, we found that PDTC/Cu complex

significantly enhanced p-JNK and pERK proteins expression, and these effects could be reversed by addition of the JNK inhibitor, SP600125, but ERK inhibitor could not. Furthermore, PDTC/Cu complex could not promote the pp38 protein expression. Thus, we concluded that PDTC/Cu complex induced p-JNK-related apoptotic signaling.

A previous study has reported that p-JNK plays an important role in induction of the mitochondrial intrinsic apoptotic pathway (*35*). Current evidence suggests that mitochondria play a pivotal role in caspase activation through the release of cytochrome *c*.(*21*). Another study also showed that mitochondrial apoptotic signaling is related to MAPKKK function within the JNK/stress-activated protein kinase (SAPK) and p38 MAPK signaling pathways (*36*). For example, it has been reported that cardiocyte apoptosis is attenuated by inhibition of JNK phosphorylation and attenuated by TNF-α, caspase-8, Bax, and cytochrome *c* through mitochondria pathway (*37*). However, there have been no studies that have explored the relationship of JNK and mitochondria in lung alveolar cells. Here, we reported that treatment with PDTC/Cu complex significantly increased Bcl-2 mRNA and protein expression in L2 cells. Furthermore, caspase-9, caspase-7, and caspase-3 activation were detected after these cells were treated with PDTC/Cu complex, and addition of a p-JNK inhibitor reversed these effects. We suggested that PDTC/Cu complex induced cell death signaling through a JNK and mitochondria dependent pathway in L2 cells.

Apoptosis is known to involve the proteolytic activation of caspase cysteine proteases, which is regulated by Bcl-2 family proteins. Bcl-2 family proteins are localized in the ER membrane and have been shown to influence ER homeostasis and ER membrane permeability. ER proteins interact with Bcl-2 family proteins to activate death effectors or influence the sensitivity of mitochondria to apoptotic transitions (*20*). Among the ER-resident molecular chaperones, Grp78 is a highly conserved 78-kDa protein that has 60% amino-acid homology with the 70-kDa heat-shock protein (HSP70). Grp94 is the most abundant glycoprotein in ER and has 50% amino-acid homology with HSP90. Both Grp78 and Grp94 have been identified as ER indicators (*37*). ATF4 is a basic leucine zipper transcription factor, and upregulation of ATF4 occurs during the recovery of cellular stress, growth arrest, and DNA damage (*38*). The transcription factor CHOP is also known as growth-arrest and DNA-damage inducible gene 153 (GADD153). This protein is a member of the C/EBP transcription factor family that heterodimerizes with other C/EBPs and can be induced by ATF4. CHOP is known to promote apoptotic cell death (*39*). In idiopathic pulmonary fibrosis, ER stress induces type II alveolar epithelial cell apoptosis through activation of ATF6, ATF4, CHOP, and X-box binding protein 1 (XBP1) (*40*). It has also been shown that anticancer drugs increase CHOP and Grp78 expression to induce ER stress-related apoptosis in A549 cells (*41*). In our experiments, we found that

PDTC/Cu complex decreased procaspase-12 and increased Grp78 and Grp94 protein expression in L2 cells. The mRNAs of Grp78, Grp94, ATF4, and CHOP were also increased by PDTC/Cu complex treatment. All of these effects could be reversed by addition of the JNK inhibitor. Thus, these results indicated that the ER stress pathway was activated by PDTC/Cu complex and that this was influenced by p-JNK.

Collectively, we presented evidence showing that PDTC/Cu complex decreased cell viability and Bcl-2 expression and increase p-JNK expression in L2 cells. Furthermore, a decrease in MMP, increased release of cytochrome *c*, and caspase-9, caspase-7, and caspase-3 activation were involved in PDTC/Cu complex-induced cell death. Furthermore, increased levels of Grp78, Grp94, ATF4, and CHOP and decreased procaspase-12 were reported in the p-JNK induced apoptotic pathway (Figure 8). These results indicated that low-dose PDTC/Cu complex exposure promoted alveolar epithelial cell apoptosis through p-JNK-dependent mitochondria and ER stress pathways.

Acknowledgement. This work was supported by research grants form the National Science Council of Taiwan (NSC 98-2314-B-039-015 and NSC 98-2815-C-039-031-B) and the China Medical University (CMU 98-N2-03), Taichung, Taiwan.

References

(1) Yamamoto, M., Toda, M., Tanaka, K., Sugita, T., Sasaki, S., Uneyama, C., and Morikawa, K. (2007). Study on usage of pesticides in various countries. *Kokuritsu. Iyakuhin. Shokuhin. Eisei. Kenkyusho. Hokoku.* 92-100.

(2) Boers, D., van Amelsvoort, L., Colosio, C., Corsini, E., Fustinoni, S., Campo, L., Bosetti, C., La Vecchia, C., Vergieva, T., Tarkowski, M., Liesivuori, J., Steerenberg, P., and van Loveren, H. (2008). Asthmatic symptoms after exposure to ethylenebisdithiocarbamates and other pesticides in the Europit field studies. *Hum. Exp. Toxicol.* **27**, 721-727.

(3) Chang, X., Shao, C., Wu, Q., Huang, M., and Zhou, Z. (2009). Pyrrolidine dithiocarbamate attenuates paraquat-induced lung injury in rats. *J. Biomed. Biotechnol.* **2009**,619487.

(4) Chuang, Y. H., Chuang, W. L., Huang, S. P., Liu, C. K., and Huang, C. H. (2009). Inhibition of nuclear factor-kappa B (NF-kappaB) activation attenuates ureteric damage in obstructive uropathy. *Pharmacol Res* **60**, 347-357.

(5) Yang, R. H., Strong, J. A., and Zhang, J. M. (2009). NF-kappaB mediated enhancement of potassium currents by the chemokine CXCL1/growth related oncogene in small diameter rat sensory neurons. *Mol. Pain.* **5**, 26.

(6) Atanasov, A. G., Tam, S., Rocken, J. M., Baker, M. E., and Odermatt, A. (2003).

Inhibition of 11 beta-hydroxysteroid dehydrogenase type 2 by dithiocarbamates. *Biochem. Biophys. Res. Commun.* **308**, 257-262.

(7) Chen, S. H., Liu, S. H., Liang, Y. C., Lin, J. K., and Lin-Shiau, S. Y. (2000). Death signaling pathway induced by pyrrolidine dithiocarbamate-$Cu^{(2+)}$ complex in the cultured rat cortical astrocytes. *Glia* **31**, 249-261.

(8) Chen, S. H., Lin, J. K., Liang, Y. C., Pan, M. H., Liu, S. H., and Lin-Shiau, S. Y. (2008). Involvement of activating transcription factors JNK, NF-kappaB, and AP-1 in apoptosis induced by pyrrolidine dithiocarbamate/Cu complex. *Eur. J. Pharmacol.* **594**, 9-17.

(9) Krewski, D., Chambers, A., Stern, B. R., Aggett, P. J., Plunkett, L., and Rudenko, L. (2010). Development of a copper database for exposure-response analysis. *J. Toxicol. Environ. Health. A.* **73**, 208-216.

(10) Stern, B. R. (2010). Essentiality and toxicity in copper health risk assessment: overview, update and regulatory considerations. *J. Toxicol. Environ. Health. A.* **73**, 114-127.

(11) Linder, M. C., and Hazegh-Azam, M. (1996). Copper biochemistry and molecular biology. *Am. J. Clin. Nutr.* **63**, 797S-811S.

(12) Ozcelik, D., and Uzun, H. (2009). Copper intoxication; antioxidant defenses and oxidative damage in rat brain. *Biol. Trace. Elem. Res.* **127**, 45-52.

(13) Yalcin, E., Talim, B., Ozcelik, U., Dogru, D., Cobanoglu, N., Pekcan, S., and Kiper, N. (2009). Does defective apoptosis play a role in cystic fibrosis lung disease? *Arch. Med. Res.* **40**, 561-564.

(14) Diab, K. J., Adamowicz, J. J., Kamocki, K., Rush, N. I., Garrison, J., Gu, Y., Schweitzer, K. S., Skobeleva, A., Rajashekhar, G., Hubbard, W. C., Berdyshev, E. V., and Petrache, I. (2010). Stimulation of Sphingosine 1 Phosphate Signaling as an Alveolar Cell Survival Strategy in Emphysema. *Am. J. Respir. Crit. Care. Med.* **181**, 344-352.

(15) Meng, G., Zhao, J., Wang, H. M., Ding, R. G., Zhang, X. C., Huan, C. Q., and uan, J. X. (2010). Cell Injuries of the Blood-Air Barrier in Acute Lung Injury Caused by Perfluoroisobutylene Exposure. *J. Occup. Health*. **52**, 48-57.

(16) Yoshida, K., Kuwano, K., Hagimoto, N., Watanabe, K., Matsuba, T., Fujita, M., Inoshima, I., and Hara, N. (2002). MAP kinase activation and apoptosis in lung tissues from patients with idiopathic pulmonary fibrosis. *J. Pathol.* **198**, 388-396.

(17) Chang, L., and Karin, M. (2001). Mammalian MAP kinase signalling cascades. *Nature* **410**, 37-40.

(18) Penna, F., Reffo, P., Muzio, G., Canuto, R. A., Baccino, F. M., Bonelli, G., and Costelli, P. (2009). Mechanisms of clofibrate-induced apoptosis in Yoshida AH-130 hepatoma cells. *Biochem. Pharmacol.* **77**, 169-176.

(19) Zhang, Y., Wang, J., Li, L., Sun, Y., and Feng, B. (2010). Three common GJB2 mutations causing nonsyndromic hearing loss in Chinese populations are retained in the endoplasmic reticulum. *Acta. Otolaryngol*. [Epub ahead of print].

(20) Breckenridge, D. G., Germain, M., Mathai, J. P., Nguyen, M., and Shore, G. C. (2003). Regulation of apoptosis by endoplasmic reticulum pathways. *Oncogene* **22**, 8608-8618.

(21) Desagher, S., and Martinou, J. C. (2000). Mitochondria as the central control point of apoptosis. *Trends. Cell. Biol.* **10**, 369-377.

(22) Lu, T. H., Chen, C. H., Lee, M. J., Ho, T. J., Leung, Y. M., Hung, D. Z., Yen, C. C., He, T. Y. and Chen, Y. W. (2010) Methylmercury chloride induces alveolar type II epithelial cell damage through an oxidative stress-related mitochondrial cell death pathway. *Toxicol Lett* **194**, 70-78.

(23) Bozec, A., Chuzel, F., Chater, S., Paulin, C., Bars, R., Benahmed, M., and Mauduit, C. (2004). The mitochondrial-dependent pathway is chronically affected in testicular germ cell death in adult rats exposed in utero to anti-androgens. *J. Endocrinol.* **183**, 79-90.

(24) Urban, P., Pavlikova, M., Sivonova, M., Kaplan, P., Tatarkova, Z., Kaminska, B., and Lehotsky, J. (2009). Molecular analysis of endoplasmic reticulum stress response after global forebrain ischemia/reperfusion in rats: effect of

neuroprotectant simvastatin. *Cell. Mol. Neurobiol.* **29**, 181-192.

(25) Pirot, P., Eizirik, D. L., and Cardozo, A. K. (2006). Interferon-gamma potentiates endoplasmic reticulum stress-induced death by reducing pancreatic beta cell defence mechanisms. *Diabetologia* **49**, 1229-1236.

(26) Cardozo, A. K., Ortis, F., Storling, J., Feng, Y. M., Rasschaert, J., Tonnesen, M., Van Eylen, F., Mandrup-Poulsen, T., Herchuelz, A., and Eizirik, D. L. (2005). Cytokines downregulate the sarcoendoplasmic reticulum pump Ca^{2+} ATPase 2b and deplete endoplasmic reticulum Ca^{2+}, leading to induction of endoplasmic reticulum stress in pancreatic beta-cells. *Diabetes* **54**, 452-461.

(27) Chen, Y. W., Huang, C. F., Tsai, K. S., Yang, R. S., Yen, C. C., Yang, C. Y., Lin-Shiau, S. Y., and Liu, S. H. (2006). Methylmercury induces pancreatic beta-cell apoptosis and dysfunction. *Chem. Res. Toxicol.* **19**, 1080-1085.

(28) Zhong, F., Zhang, S., Shao, C., Yang, J., and Wu, X. (2009). Arsenic Trioxide Inhibits Cholangiocarcinoma Cell Growth and induces Apoptosis. *Pathol. Oncol. Res*. [Epub ahead of print].

(29) Putcha, G. V., Harris, C. A., Moulder, K. L., Easton, R. M., Thompson, C. B., and Johnson, E. M., Jr. (2002). Intrinsic and extrinsic pathway signaling during neuronal apoptosis: lessons from the analysis of mutant mice. *J. Cell. Biol.* **157**, 441-453.

(30) Waisberg, D. R., Barbas-Filho, J. V., Parra, E. R., Fernezlian, S., de Carvalho, C. R., Kairalla, R. A., and Capelozzi, V. L. (2010). Abnormal expression of telomerase/apoptosis limits type II alveolar epithelial cell replication in the early remodeling of usual interstitial pneumonia/idiopathic pulmonary fibrosis. *Hum Pathol* **41**, 385-391.

(31) Yang, L., Yan, D., Yan, C., and Du, H. (2003). Peroxisome proliferator-activated receptor gamma and ligands inhibit surfactant protein B gene expression in the lung. *J. Biol. Chem.* **278**, 36841-36847.

(32) Dinh, C. T., and Van De Water, T. R. (2009). Blocking pro-cell-death signal pathways to conserve hearing. *Audiol. Neurootol.* **14**, 383-392.

(33) Mizote, I., Yamaguchi, O., Hikoso, S., Takeda, T., Taneike, M., Oka, T., Tamai, T., Oyabu, J., Matsumura, Y., Nishida, K., Komuro, I., Hori, M., and Otsu, K. (2010). Activation of MTK1/MEKK4 induces cardiomyocyte death and heart failure. *J. Mol. Cell. Cardiol.* **48**, 302-309.

(34) Engstrom, W., Ward, A., and Moorwood, K. (2010). The role of scaffold proteins in JNK signalling. *Cell. Prolif.* **43**, 56-66.

(35) Dhanasekaran, D. N., and Reddy, E. P. (2008). JNK signaling in apoptosis. *Oncogene* **27**, 6245-6251.

(36) Chang, H. Y., Nishitoh, H., Yang, X., Ichijo, H., and Baltimore, D. (1998).

Activation of apoptosis signal-regulating kinase 1 (ASK1) by the adapter protein Daxx. *Science* **281**, 1860-1863.

(37) Zhang, G. M., Wang, Y., Li, T. D., Zhang, D. W., Liu, X. H., and Yang, F. F. (2009). Change of JNK MAPK and its influence on cardiocyte apoptosis in ischemic postconditioning. *Zhejiang. Da. Xue. Xue. Bao. Yi. Xue. Ban.* **38**, 611-619.

(38) Whitney, M. L., Jefferson, L. S., and Kimball, S. R. (2009). ATF4 is necessary and sufficient for ER stress-induced upregulation of REDD1 expression. *Biochem. Biophys. Res. Commun.* **379**, 451-455.

(39) Szegezdi, E., Logue, S. E., Gorman, A. M., and Samali, A. (2006). Mediators of endoplasmic reticulum stress-induced apoptosis. *EMBO. Rep.* **7**, 880-885.

(40) Korfei, M., Ruppert, C., Mahavadi, P., Henneke, I., Markart, P., Koch, M., Lang, G., Fink, L., Bohle, R. M., Seeger, W., Weaver, T. E., and Guenther, A. (2008). Epithelial endoplasmic reticulum stress and apoptosis in sporadic idiopathic pulmonary fibrosis. *Am. J. Respir. Crit. Care. Med.* **178**, 838-846.

(41) Lin, S. S., Huang, H. P., Yang, J. S., Wu, J. Y., Hsia, T. C., Lin, C. C., Lin, C. W., Kuo, C. L., Gibson Wood, W., and Chung, J. G. (2008). DNA damage and endoplasmic reticulum stress mediated curcumin-induced cell cycle arrest and apoptosis in human lung carcinoma A-549 cells through the activation caspases

cascade- and mitochondrial-dependent pathway. *Cancer. Lett.* **272**, 77-90.

Figure Legends

Figure 1. Effects of PDTC, $CuCl_2$, and PDTC/Cu complex on cell viability in lung epithelial cell-derived L2 cells. Cells were treated with $CuCl_2$ (0 to 3 μM) with or without PDTC (0, 0.5, or 1 μM) for 24 h. The cell viability was determined via MTT assay. All data are presented as means ± SEM from four independent experiments performed in triplicate. *P <0.05 as compared to vehicle control.

Figure 2. Intracellular copper contents in PDTC, $CuCl_2$, and PDTC/Cu complex exposed lung epithelial cell-derived L2 cells. Cells were treated with PDTC (0.5 μM), or $CuCl_2$ (1 μM) with or without PDTC for 24 h. Intracellular copper contents were determined by Inductively coupled plasma mass spectrometry (ICP-MS). All data are presented as means ± SEM from eight independent experiments performed in triplicate. *P <0.05 as compared to vehicle control.

Figure 3. Effects of PDTC, $CuCl_2$, and PDTC/Cu complex on caspase-9, caspase-7 and caspase-3 proteins expression in lung epithelial cell-derived L2 cells. Cells were treated with PDTC (0.5 μM), or $CuCl_2$ (1 μM) with or without PDTC for various time point. The Western blot analysis was used to detect (A) caspase-9, (B) caspase-7 and (C) caspase-3 proteins expression in lung epithelial cell-derived L2 cells. All data are

representative of three independent experiments.

Figure 4. Effects of PDTC, $CuCl_2$, and PDTC/Cu complex on MAPKs proteins expression in lung epithelial cell-derived L2 cells. Cells were pretreated with JNK inhibitor (SP600125), ERK inhibitor (PD98059), and p38 inhibitor (SB203580) for 30 min, respectively. After, cells were treated with PDTC (0.5 μM), or $CuCl_2$ (1 μM) with or without PDTC for 1 h, the MAPKs proteins, including pJNK, pERK, and pp38, were analyzed by Western blot. All data are representative of three independent experiments.

Figure 5. Effects of PDTC, $CuCl_2$, and PDTC/Cu complex on caspases proteins expression in lung epithelial cell-derived L2 cells. Cells were pretreated with JNK inhibitors, SP600125 (10 μM), or transfected with human MAPK8 short hairpin RNA (shRNA). After, cells were treated with PDTC (0.5 μM), or $CuCl_2$ (1 μM) combined with or without PDTC for 1 h. The Western blot analysis was used to detect (A) caspase-9, (B) caspase-7 and (C) caspase-3 proteins expression in lung epithelial cell-derived L2 cells. All data are representative of three independent experiments.

Figure 6. Bcl-2 mRNA and protein expression, mitochondria transmembrane potential

(MMP), and cytochrome *c* release in PDTC, $CuCl_2$, and PDTC/Cu complex treated L2 cells. (A) Cells were treated with PDTC (0.5 μM), $CuCl_2$ (1 μM), or PDTC/Cu complex with or without addition of the JNK inhibitor, SP600125 (10 μM), for 6 h, or with or without transfection of human MAPK8 short hairpin RNA (shRNA). (a) Bcl-2 mRNA and (b) protein expression were determined by quantitative real-time PCR and Western blot analysis, respectively. (B) Cells were treated as above, and flow cytometry was used to detect alterations in MMP. (C) After cells were treated as above, their cytosolic fractions were separated and cytochrome *c* release was determined via Western blot analysis. Data in (A-a) and (B) are expressed as mean ± SEM (n=4 for each group). ***P* < 0.05 as compared with vehicle control group. Data in (A-b) and (C) are representative of three independent experiments.

Figure 7. Effects of PDTC, $CuCl_2$, and PDTC/Cu complex on Grp78, Grp94, and procaspase-12 protein expression in L2 cells. Cells were treated with PDTC (0.5 μM), $CuCl_2$ (1 μM), or PDTC/Cu complex for 8–24 h and then assayed via Western blot analysis to determine procaspase-12, Grp78, and Grp94 protein levels. All data are representative of three independent experiments.

Figure 8. The mRNA expression of Grp78, Grp94, ATF4, and CHOP in PDTC, $CuCl_2$,

and PDTC/Cu complex treated L2 cells. Cells were pretreated with the JNK inhibitor, SP600125, for 30 min and then treated with PDTC (0.5 μM), $CuCl_2$ (1 μM), or PDTC/Cu complex for 24 h. mRNA levels were determined by quantitative real-time PCR. All data are expressed as mean ± SEM (n = 4 for each group). $*P < 0.05$ as compared to the vehicle control group.

Figure 9. Schematic representation of the proposed intracellular signaling leading to PDTC-Cu complex-induced cell death in alveolar lung epithelial cells.

Fig. 1.

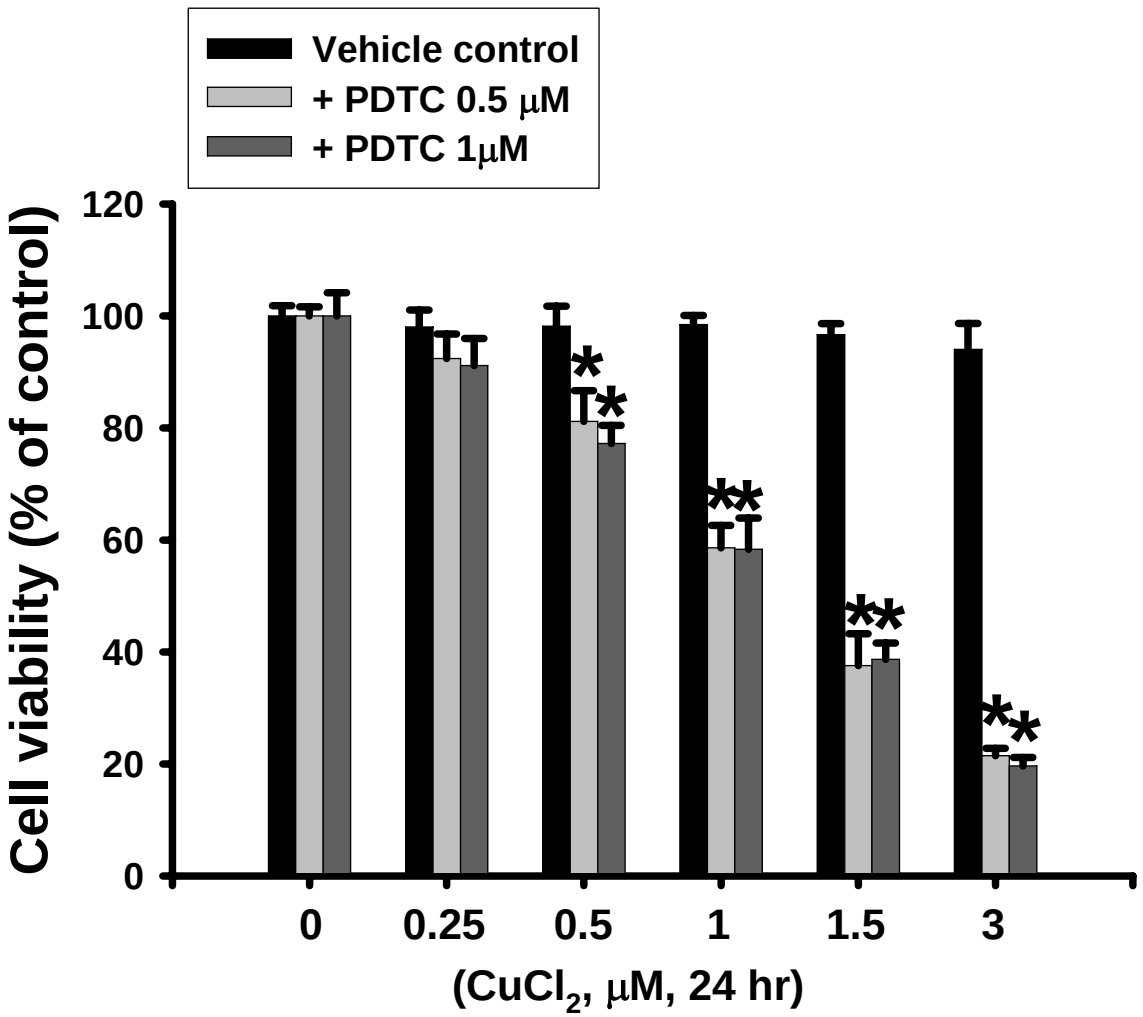
Vehicle control
+ PDTC 0.5 μM
+ PDTC 1μM
Cell viability (% of control)
120
100
80
60
40
20
0
*
*
**
**
**
0
0.25
0.5
1
1.5
3
(CuCl2, μM, 24 hr)

Fig. 2.

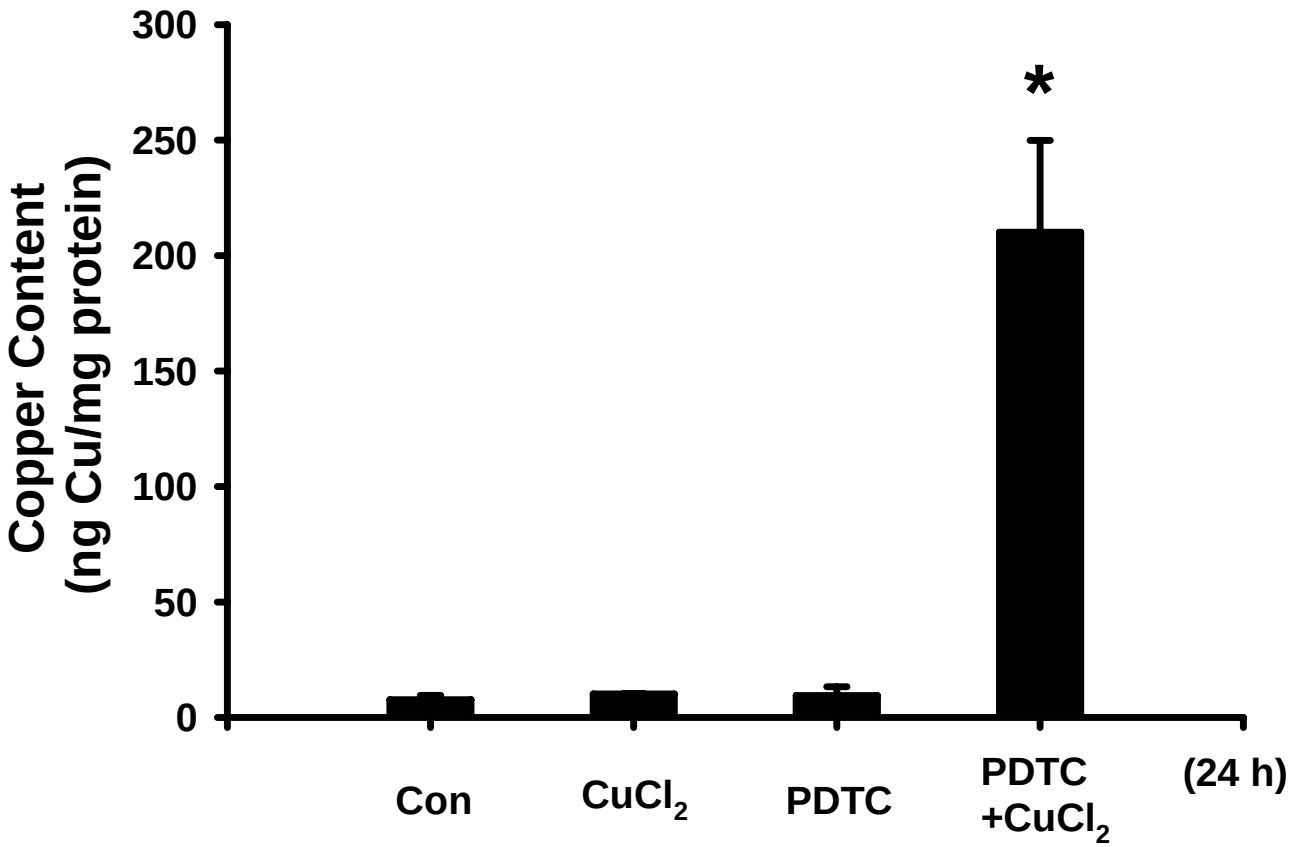
Copper Content
(ng Cu/mg protein)
300
250
200
150
100
50
0
*
Con
CuCl2
PDTC
PDTC
+CuCl2
(24 h)

Fig. 3.

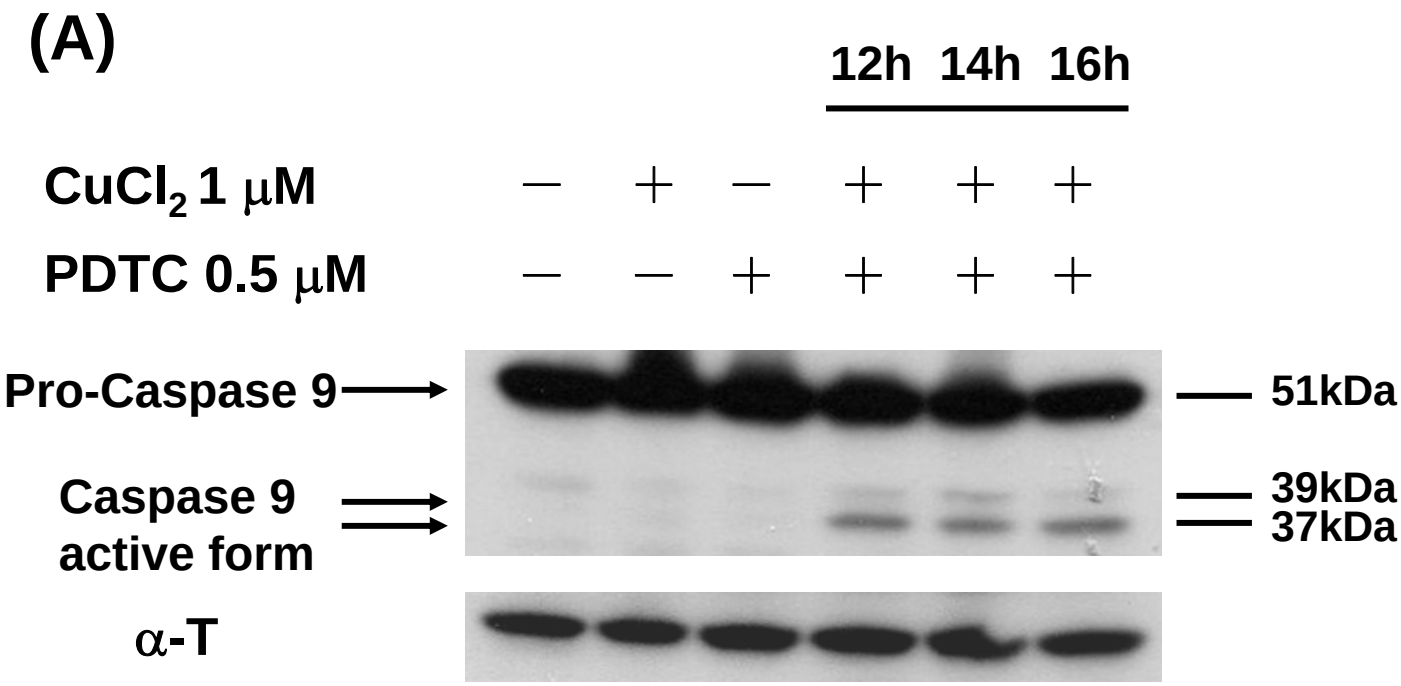
(A)
12h 14h 16h
CuCl2 1 μM
PDTC 0.5 μM
Pro-Caspase 9
Caspase 9
active form
α-T
51kDa
39kDa
37kDa

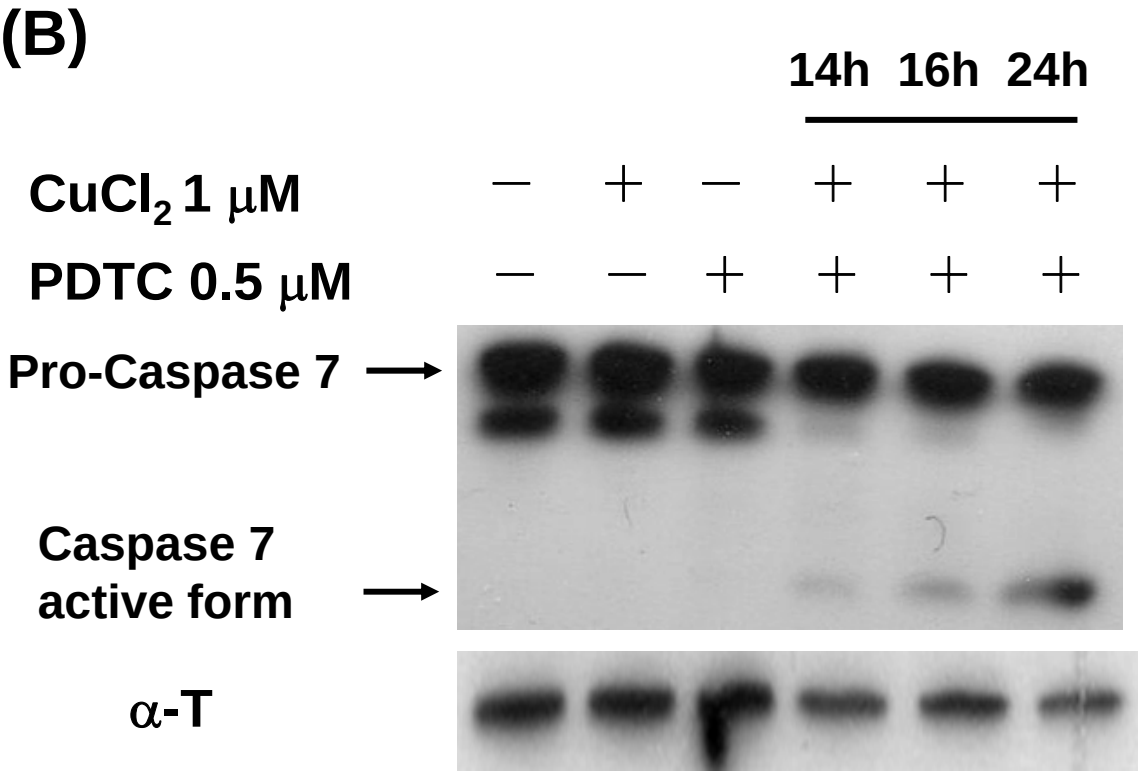
(B)
14h 16h 24h
CuCl2 1 μM
PDTC 0.5 μM
Pro-Caspase 7
Caspase 7
active form
α-T

(C)

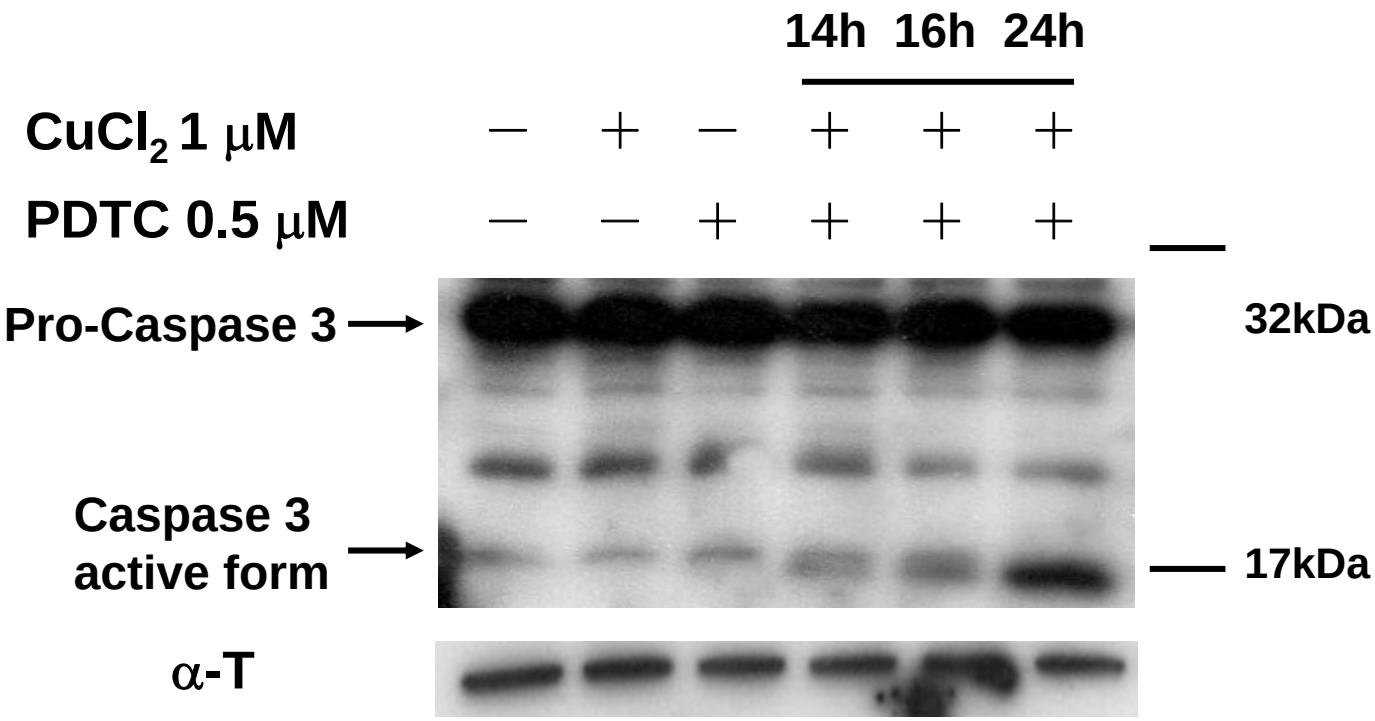
14h 16h 24h
CuCl2 1 μM
PDTC 0.5 μM
Pro-Caspase 3
Caspase 3 active form
α-T
32kDa
17kDa

Fig. 4.

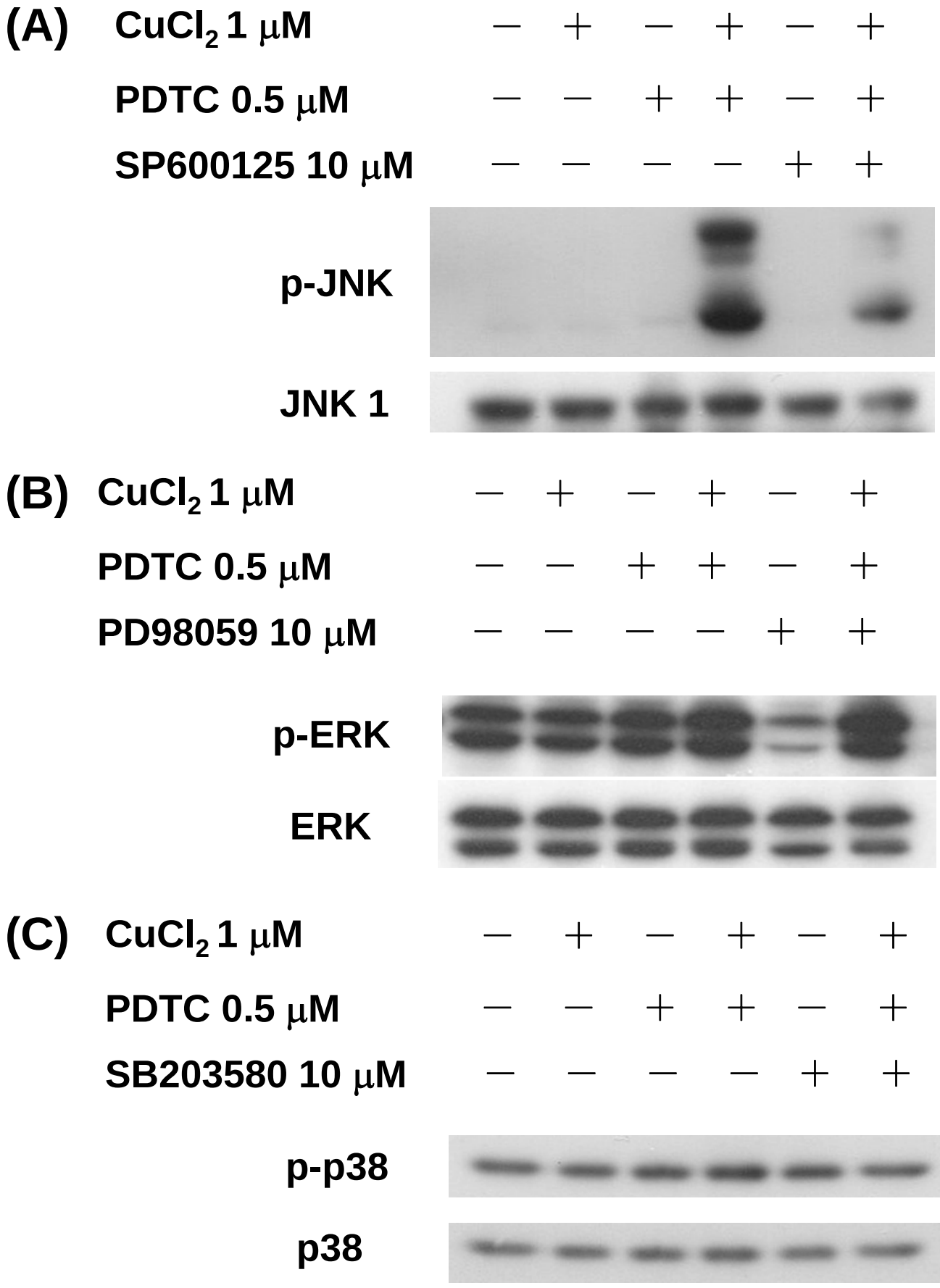
(A)
CuCl2 1 μM
PDTC 0.5 μM
SP600125 10 μM
p-JNK
JNK 1
(B)
CuCl2 1 μM
PDTC 0.5 μM
PD98059 10 μM
p-ERK
ERK
(C)
CuCl2 1 μM
PDTC 0.5 μM
SB203580 10 μM
p-p38
p38

Fig. 5.

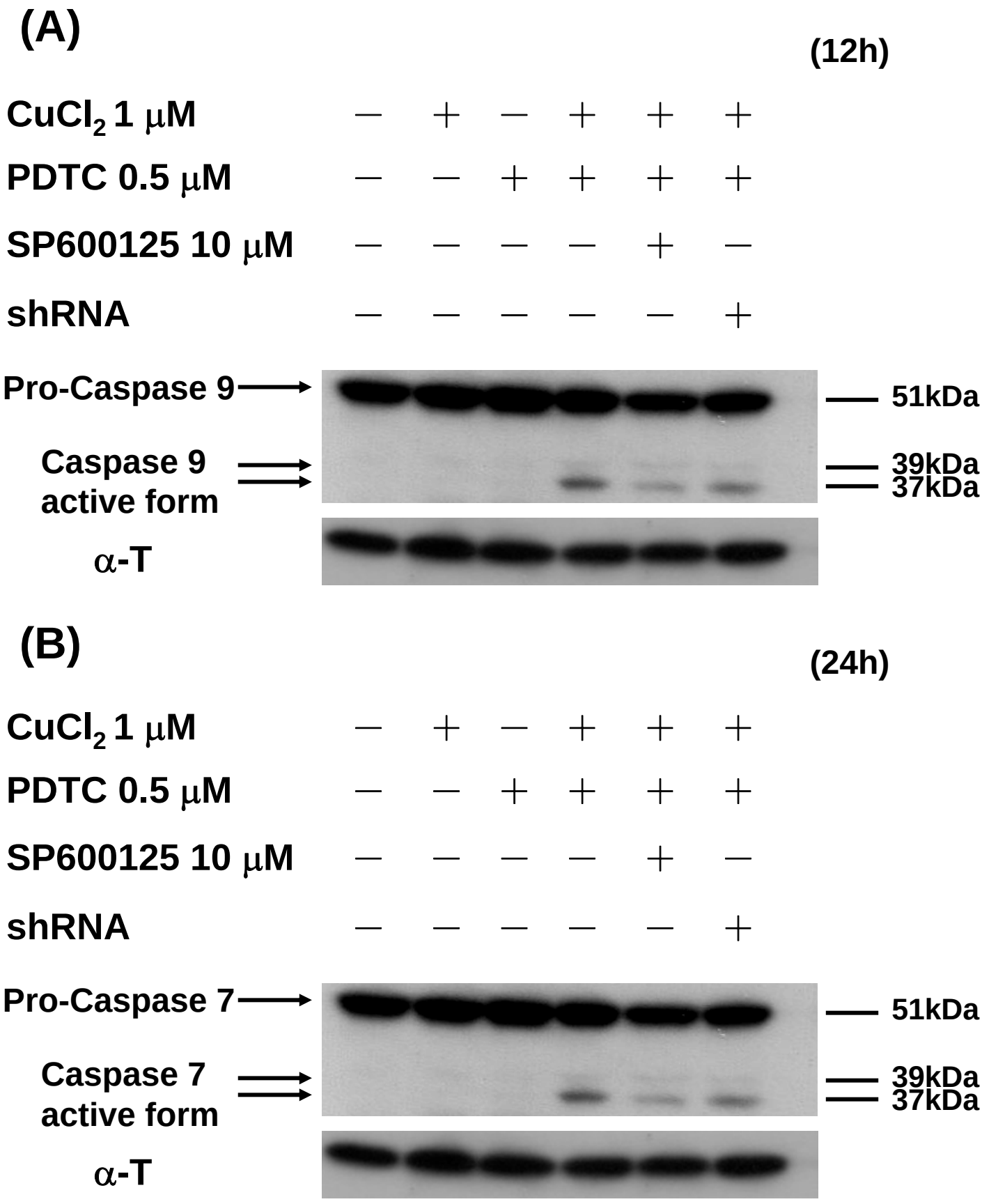
(A)
(12h)
CuCl2 1 μM
PDTC 0.5 μM
SP600125 10 μM
shRNA
Pro-Caspase 9
Caspase 9
active form
α-T
51kDa
39kDa
37kDa
(B)
(24h)
CuCl2 1 μM
PDTC 0.5 μM
SP600125 10 μM
shRNA
Pro-Caspase 7
Caspase 7
active form
α-T
51kDa
39kDa
37kDa

(C)

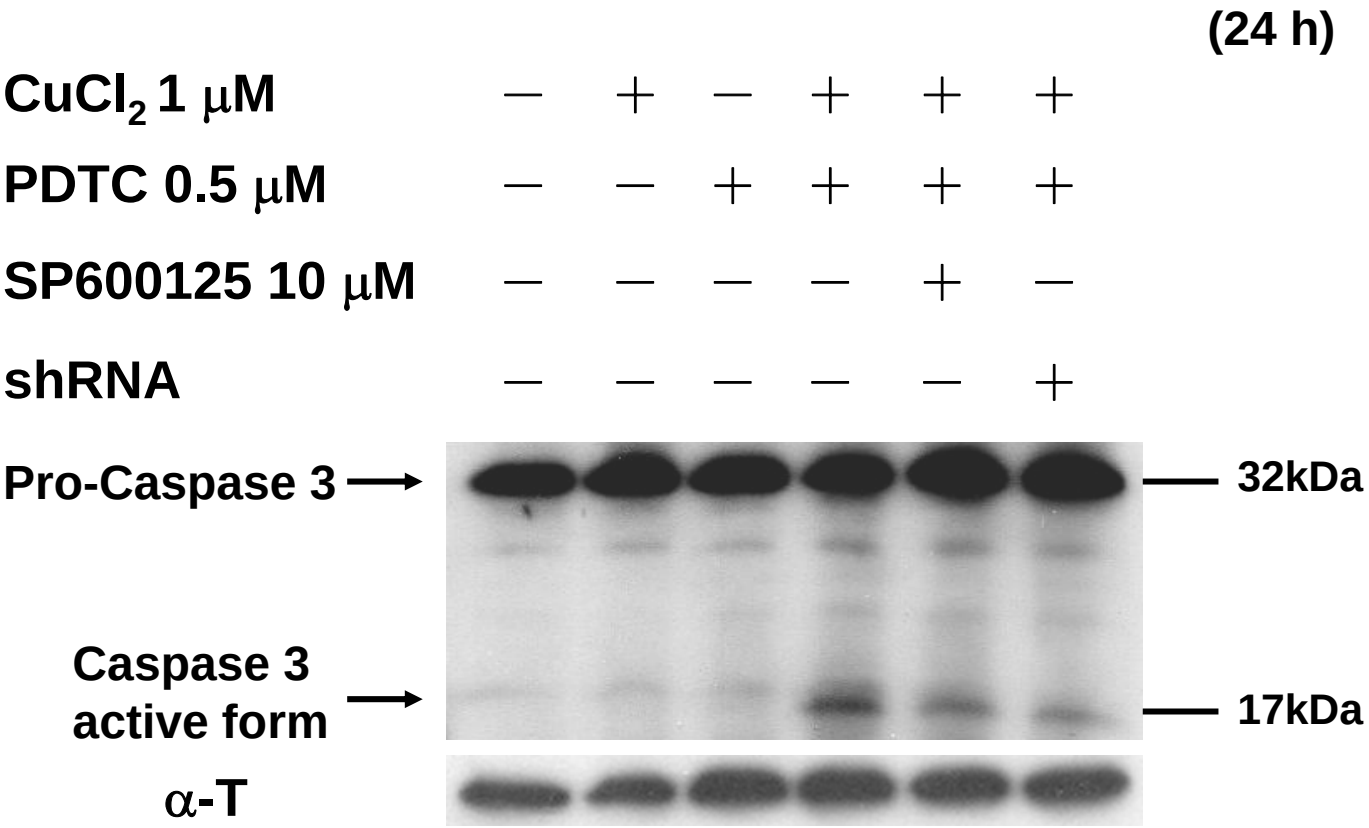
(24 h)
CuCl2 1 μM
PDTC 0.5 μM
SP600125 10 μM
shRNA
Pro-Caspase 3
Caspase 3 active form
α-T
32kDa
17kDa

Fig. 6.

(A)

(a)

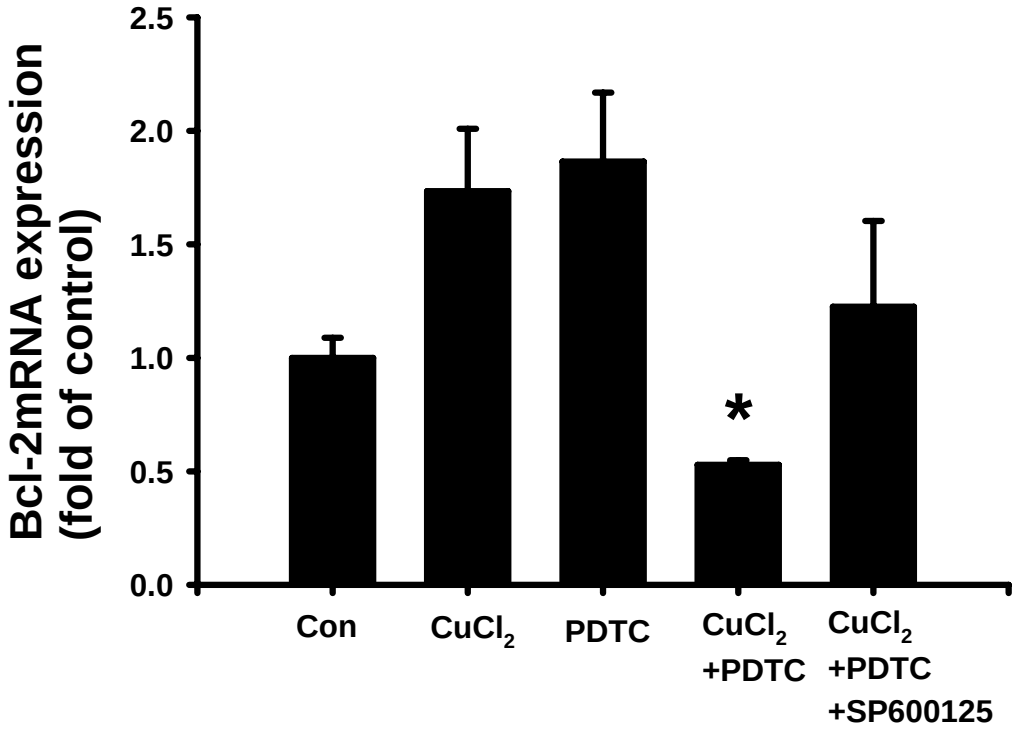
Bcl-2mRNA expression
(fold of control)
2.5
2.0
1.5
1.0
0.5
0.0
*
Con
CuCl2
PDTC
CuCl2 +PDTC
CuCl2 +PDTC +SP600125

(b)

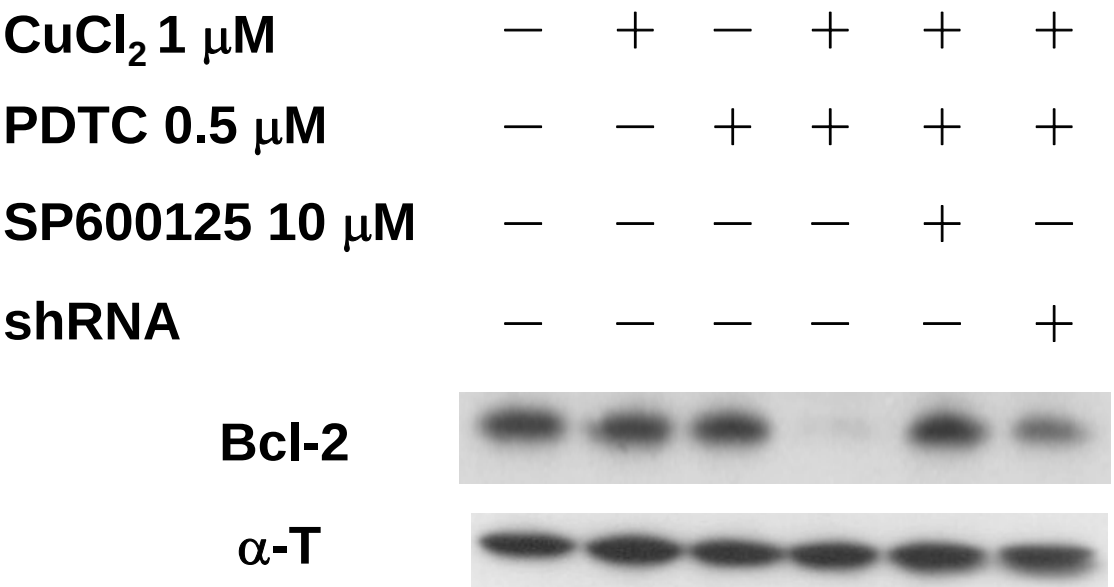
CuCl2 1 μM
PDTC 0.5 μM
SP600125 10 μM
shRNA
Bcl-2
α-T

(B)

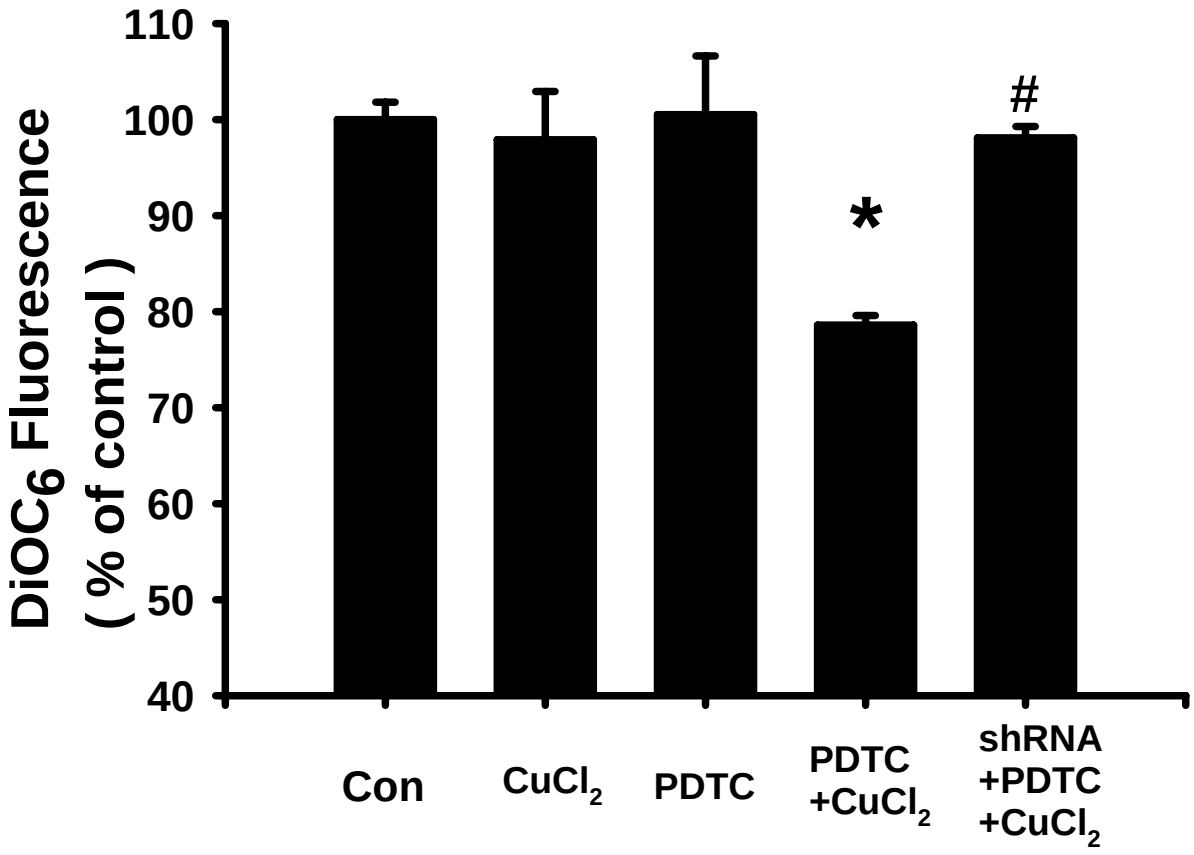
110
100
90
80
70
60
50
40
DiOC6 Fluorescence
(% of control)
*
#
Con
CuCl2
PDTC
PDTC
+CuCl2
shRNA
+PDTC
+CuCl2

(C)

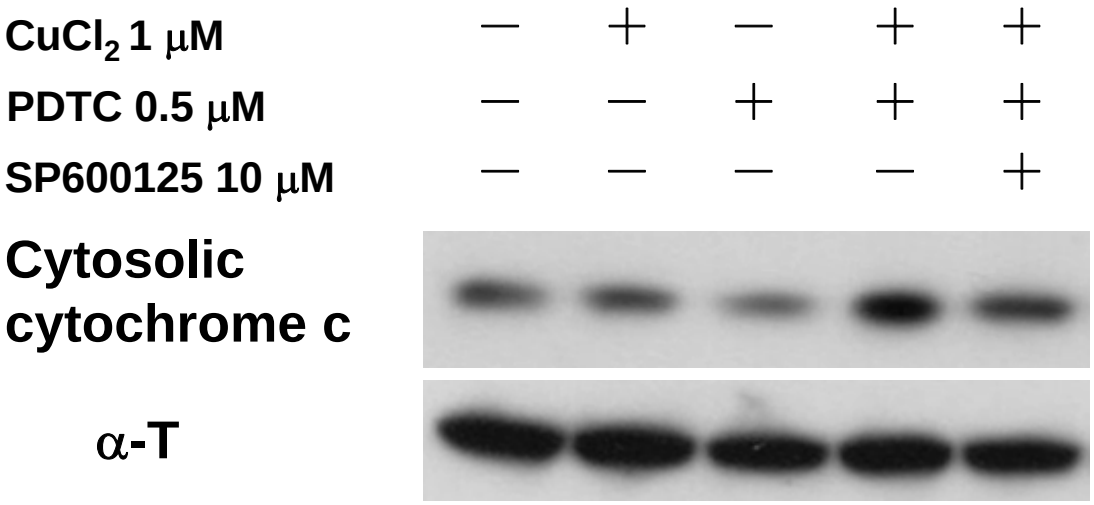
CuCl2 1 μM
PDTC 0.5 μM
SP600125 10 μM
Cytosolic
cytochrome c
α-T

Fig. 7.

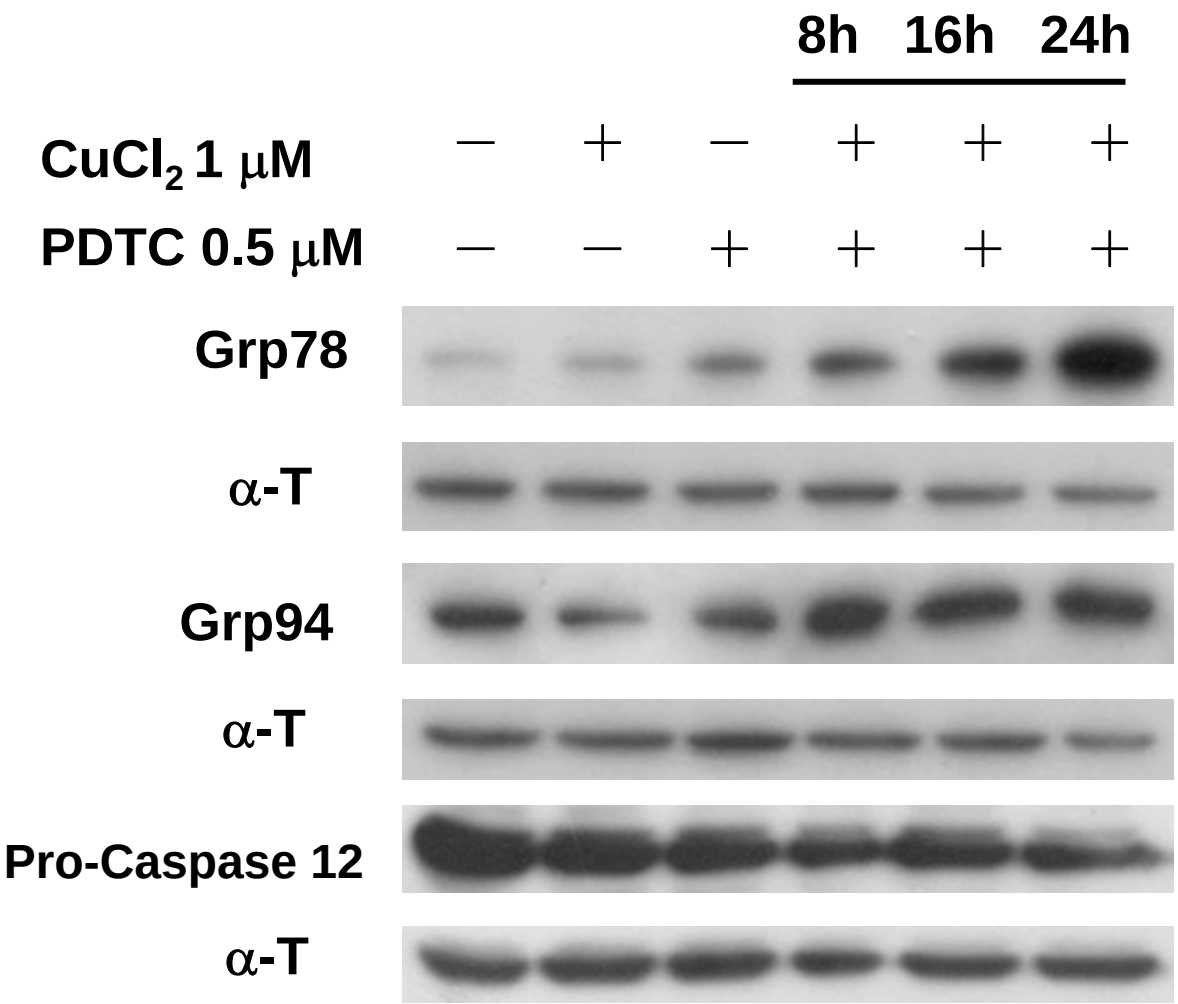
8h
16h
24h
CuCl2 1 μM
PDTC 0.5 μM
Grp78
α-T
Grp94
α-T
Pro-Caspase 12
α-T

Fig. 8.

(A)

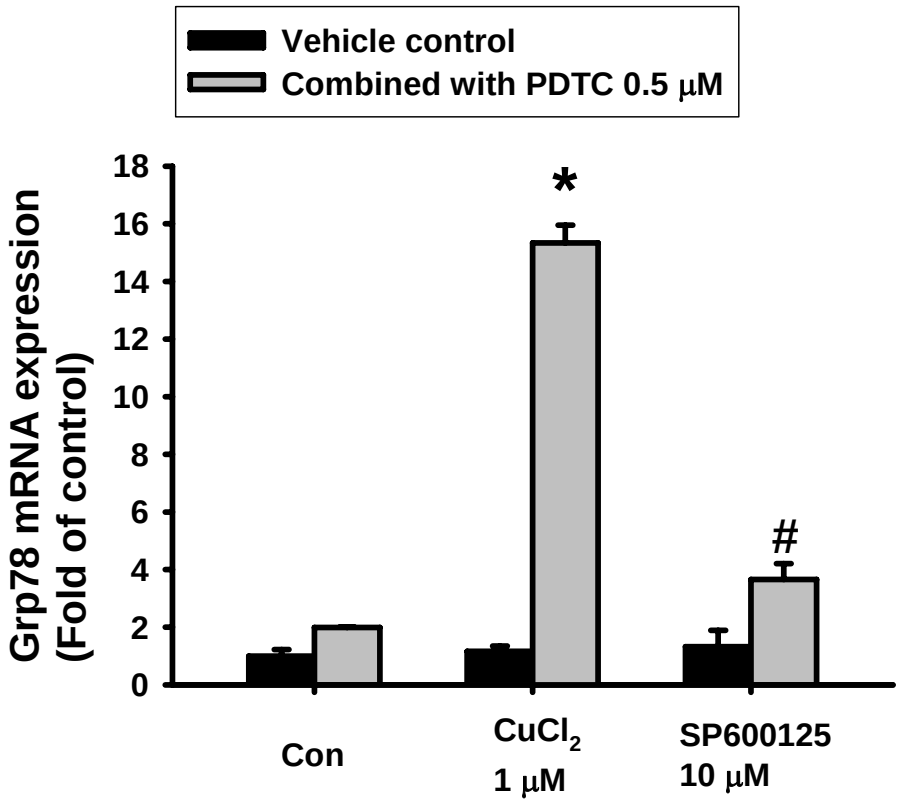
Vehicle control
Combined with PDTC 0.5 μM
Grp78 mRNA expression
(Fold of control)
18
16
14
12
10
8
6
4
2
0
*
#
Con
CuCl2
1 μM
SP600125
10 μM

(B)

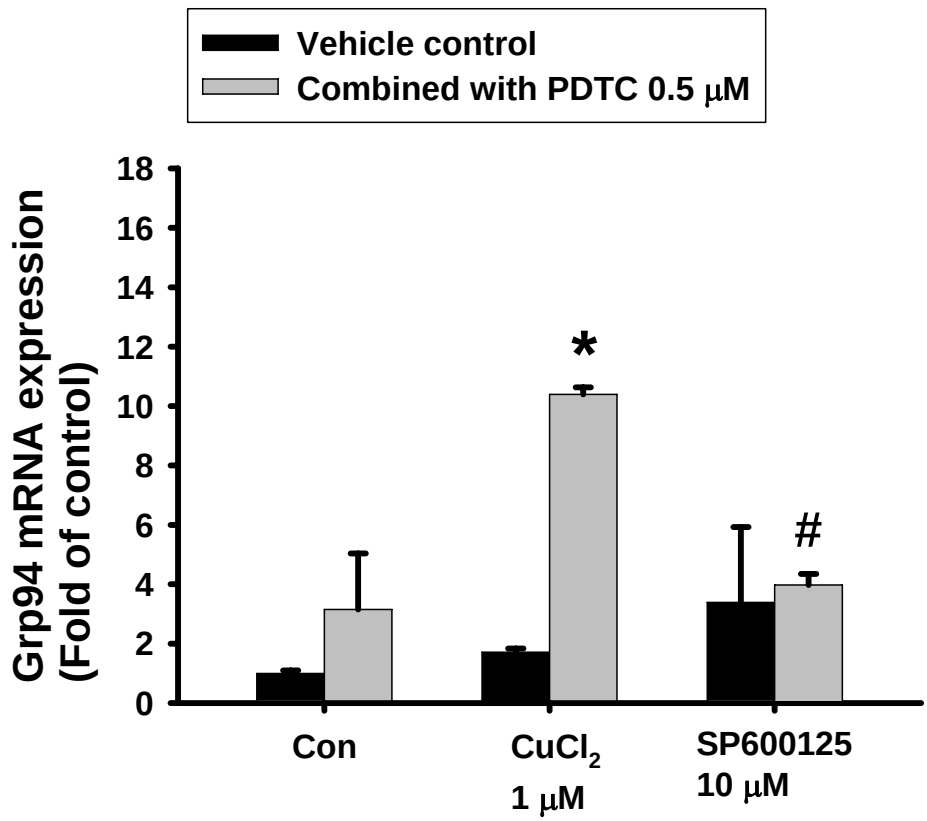
Vehicle control
Combined with PDTC 0.5 μM
Grp94 mRNA expression
(Fold of control)
18
16
14
12
10
8
6
4
2
0
*
#
Con
CuCl2
1 μM
SP600125
10 μM

(C)

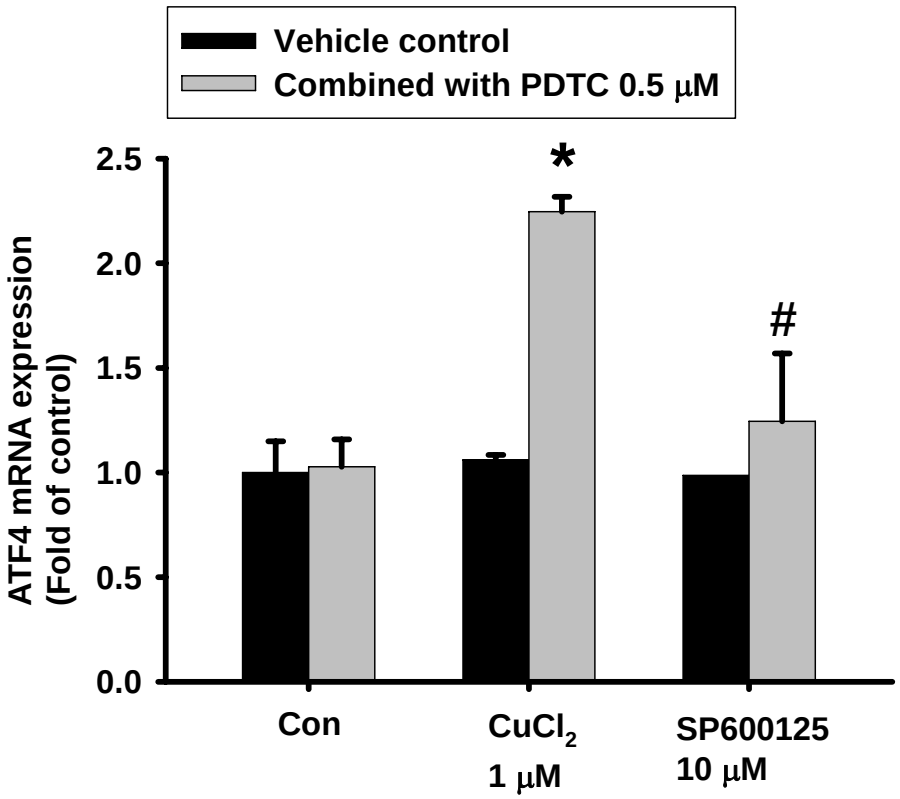
Vehicle control
Combined with PDTC 0.5 μM
ATF4 mRNA expression
(Fold of control)
2.5
2.0
1.5
1.0
0.5
0.0
*
#
Con
CuCl2
1 μM
SP600125
10 μM

(D)

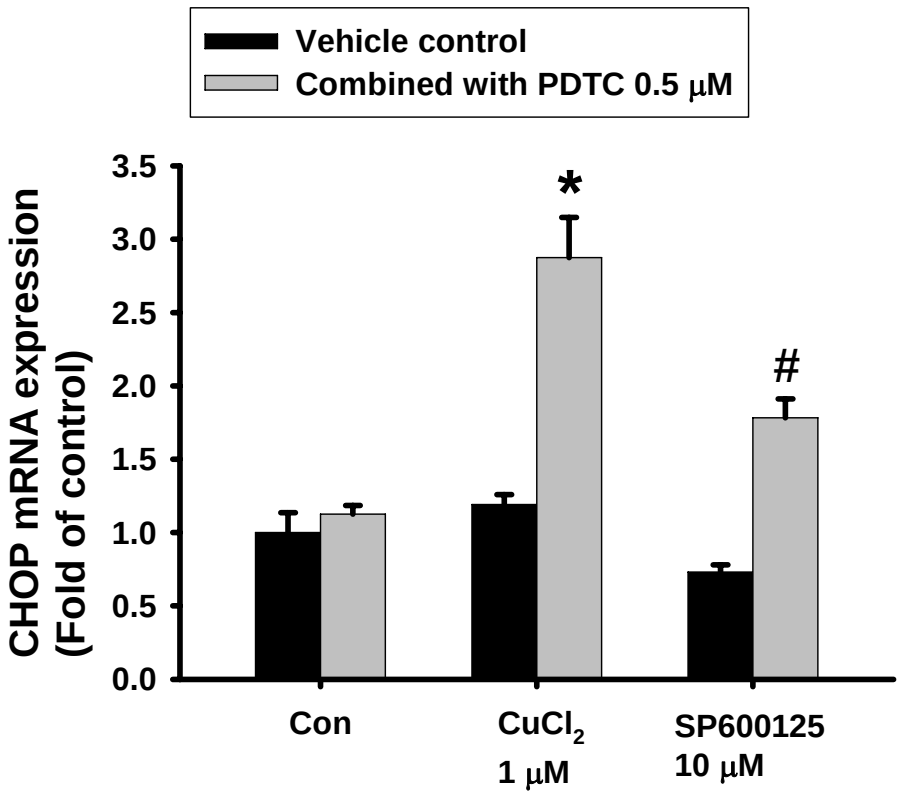
Vehicle control
Combined with PDTC 0.5 μM
CHOP mRNA expression
(Fold of control)
3.5
3.0
2.5
2.0
1.5
1.0
0.5
0.0
*
#
Con
CuCl2
1 μM
SP600125
10 μM

Fig. 9.

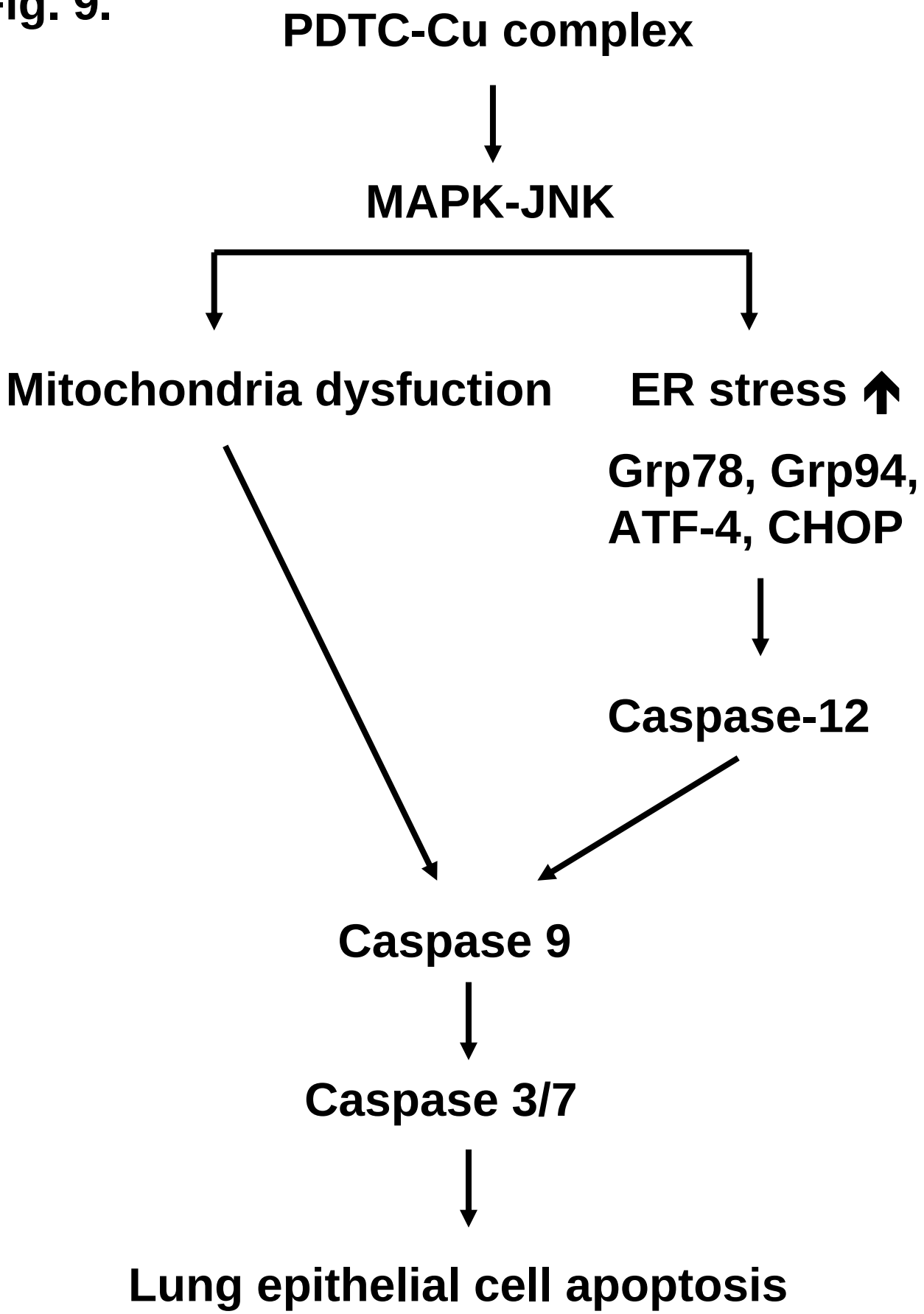
PDTC-Cu complex
MAPK-JNK
Mitochondria dysfuction
ER stress
Grp78, Grp94,
ATF-4, CHOP
Caspase-12
Caspase 9
Caspase 3/7
Lung epithelial cell apoptosis